Visible-Laser Acceleration of Relativistic Electrons in a Semi-Infinite Vacuum

T. Plettner and R. L. Byer

Stanford University, Stanford, California 94305, USA

E. Colby, B. Cowan, C. M. S. Sears, J. E. Spencer, and R. H. Siemann

SLAC, Menlo Park, California 94025, USA

We demonstrate a new particle acceleration mechanism using 800 nm laser radiation to accelerate relativistic electrons in a semi-infinite vacuum. The experimental demonstration is the first of its kind and is a proof of principle for the concept of laser-driven particle acceleration in a structure loaded vacuum. We observed up to 30 keV energy modulation over a distance of 1000λ, corresponding to a 40 MeV/m peak gradient. The energy modulation was observed to scale linearly with the laser electric field and showed the expected laser-polarization dependence. Furthermore, as expected, laser acceleration occurred only in the presence of a boundary that limited the laser-electron interaction to a finite distance.

New technologies have played a critical role in the evolution of particle accelerators [1]. Laser-driven particle acceleration in vacuum has been proposed as a future candidate particle acceleration scheme with potential for substantially increased accelerator gradients. Numerous designs for laser-driven particle accelerator structures, which range from wave-guiding schemes to semiopen free-space structures, have been proposed and analyzed at a theoretical level. Our proof-of-principle experiment demonstrates this new laser acceleration mechanism that requires neither plasma, gas, nor wiggler to achieve energy coupling.

The proof-of-principle demonstration was carried out with the simplest possible configuration that allows testing the key physics. We employed a single Gaussian laser beam terminated by a single downstream boundary, resembling a configuration originally proposed by Edinghofer and Pantell [2]. Figure 1 illustrates the laser and electron beam configuration used in the proof-of-principle experiment.

As depicted in Fig. 1 the propagation axis z' of the laser is oriented at an angle α to the propagation axis z of the electron. The accelerating longitudinal electric field component $E_z(z)$ results from the component of the laser electric field parallel to the electron beam axis. An analytical expression for $E_z(z)$ resulting from a pair of crossed Gaussian beams has been calculated by Esarey, Sprangle, and Krall [3]. For the case of a single laser beam, this $E_z(z)$ expression is reduced by a factor of $1/2$. The energy gain of the electron corresponds to the integral of $E_z(z)$ over the interaction length of an electron beam with the laser beam. However, in such a free space configuration the phase velocity of the laser beam is not matched to the velocity of the electrons, and in accordance to the Lawson-Woodward theorem [4] the acceleration integrates to zero when the laser-electron interaction proceeds to infinity. The presence of a boundary limits the laser beam interac-

tion with the electron beam and allows for a nonzero energy exchange of the field with the electrons [5].

As pointed out by Huang, Stupakov, and Zolotorev [6] the energy gain found from the path integral of $E_z(z)$ is equivalent to the energy gain predicted by inverse transition radiation, which corresponds to the overlap integral of the laser field and the transition radiation from the boundary. However, because of its simplicity, we employ the former calculation method for the energy gain estimates in this article.

Table I lists the key laser and electron beam parameters used in the experiment. The electron beam traversed an 8 μm thick gold coated Kapton tape, which was illuminated at laser pulse energies above the damage threshold fluence of the 0.9 μm thick reflective gold coating. The laser beam fluences at which a modulation effect was visible ranged between 1 and 5 J/cm^2. The precise evolution of the material ablation depends on an array of factors, such as the air-vacuum environment, the type of material, and the laser pulse properties. However, since the electron
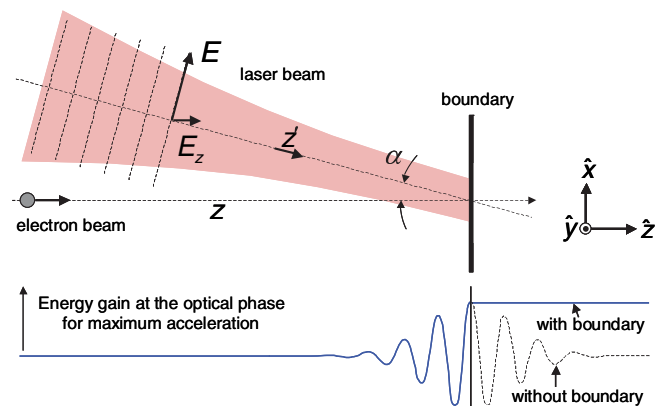

FIG. 1 (color).   The laser beam, electron beam, and boundary configuration.

TABLE I. Experimental parameters.

Laser beam parameters	
Laser wavelength	800 nm
Laser FWHM pulse duration	4 ps
Laser FWHM waist spot size	110 μm
Laser pulse energy	0–1/2 mJ/pulse
Laser crossing angle	16 mrad
Laser polarization	Linear
Electron beam parameters	
Typical beam energy	30 MeV
FWHM electron spot size	50 μm
Typical initial FWHM energy spread	15 keV
Typical FWHM bunch length	2 ps
Typical bunch charge	<10 pC/bunch

bunch and the laser pulse have a few-ps duration, only the very initial phase of the ablation process has a potential effect on the electron beam. It is known that for the ablation of metals from ultrashort laser pulses no free plasma has developed during the laser pulse and heat diffusion into the material is negligible [7]; hence the material retains its surface morphology during that time. Reflectance measurements carried out by us confirmed the high reflectance of the gold coated Kapton tape for ablating laser pulse durations of up to 10 ps and showed a reflected spot with a similar profile to the incident spot, allowing us to establish that indeed the surface is momentarily preserved. Our measurements indicate that at most 20% of the incident laser pulse penetrated the Kapton medium.

Inside the Kapton medium (index of refraction $\eta \sim$ 1.66) the slippage distance is 1.1 μm, and assuming that 20% of the laser power is transmitted into the medium, we estimate an upper limit of 15 eV from possible inverse Cherenkov acceleration (ICA). The keV energy modulations we observe cannot be accounted for by ICA in the Kapton medium.

A high resolution 90° bending magnet located downstream of the laser-electron interaction region was employed to observe the energy spectrum of the electron beam. Since the electron beam was not optically bunched, the electron beam was spread over all possible laser optical phases, and hence the laser-driven particle acceleration effect manifested itself as an increase of the energy spread of the electron beam in the presence of the laser beam. Figure 2 shows the observed electron bunch energy broadening at optimum overlap with the laser beam.

The energy modulation for a particular laser-on event was characterized by the quadrature deviation, defined as $M_i = \sqrt{F_i^2 - \bar{F}_{\text{off}}^2}$, where F_i is the FWHM energy spread of the ith laser-on event and $\bar{F}_{\text{off}}$ is the average FWHM energy spread of the laser-off events. A simple particle tracking MATLAB code was employed to find the relation between the quadrature deviation and the corresponding peak energy modulation. The code utilized experimentally recorded laser-off energy spectra to describe the initial energy profile of the electron beam. Since the laser beam was twice as large as the electron beam, the simulation model assumed a spatially uniform laser field. The temporal structure of the laser and the electron beam were modeled with Gaussian profiles. Electrons were assumed to be evenly distributed over all optical phases of the laser beam. At the condition of best temporal overlap the model found that $M_i = 2.2 E_{\text{peak}}$, where E_{peak} is the peak energy gain caused by the laser-driven particle acceleration.
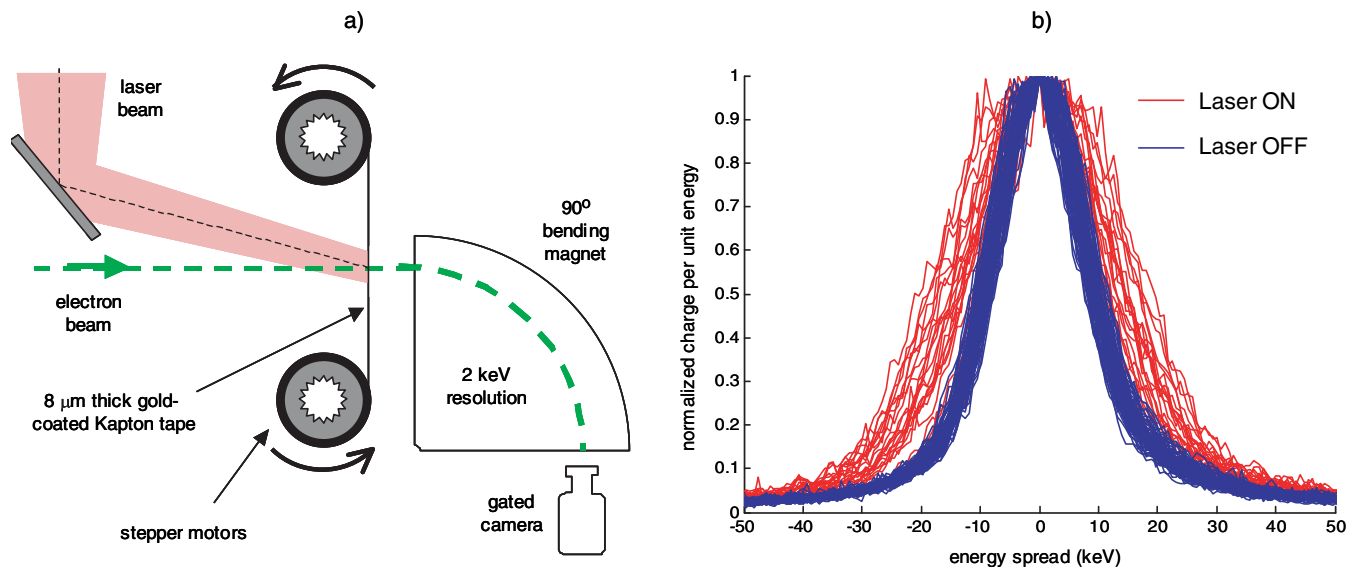

FIG. 2 (color).   (a) Layout of the experiment. The tape was moved to a new, not-yet damaged surface for each laser shot. (b) Experimentally observed laser-driven energy modulation.
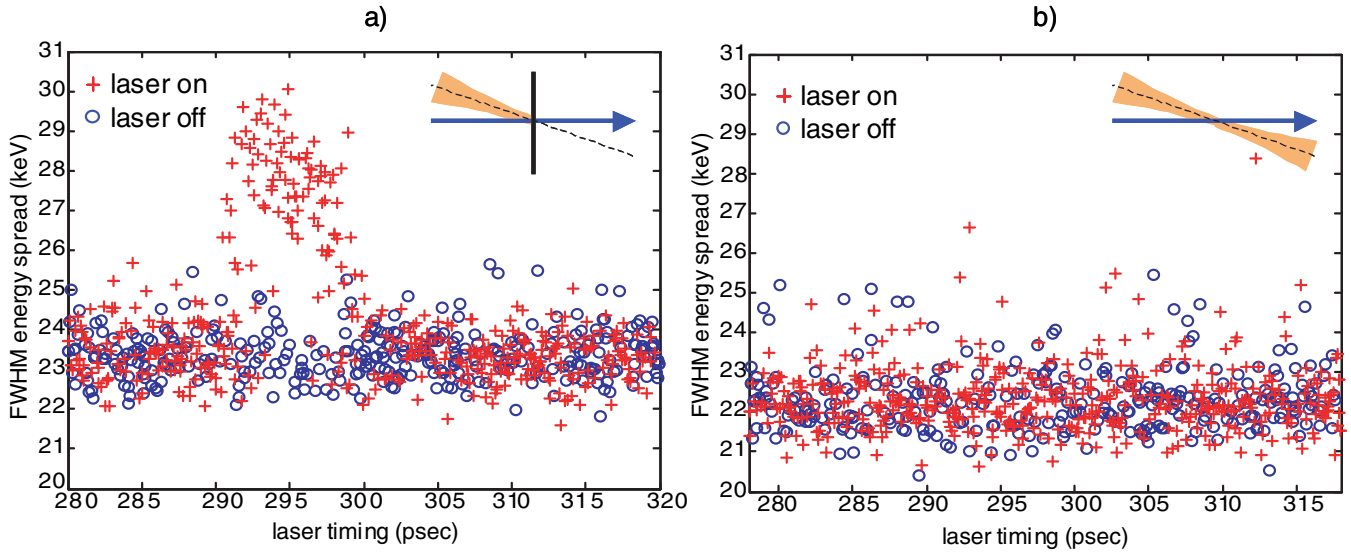
FIG. 3 (color).   The experimental confirmation of the Lawson-Woodward theorem.

Because of the low bunch charge, space charge effects were not included.

As can be observed in Fig. 3(a) shot-to-shot jitter in the electron bunch timing introduced significant fluctuations in the observed M_i. To mitigate this, an average energy modulation $\langle M \rangle = \sum_i M_i / N$, $|T - t_i| \leq \delta$, where $\delta = 1$ ps, T is the timing of optimum modulation, and N the number of events (usually $N \sim 50$) was used to compute the average. The observed average energy modulation $\langle M \rangle$ was approximately $1/2$ the value of the largest observed modulation events, which were close to the theoretically calculated peak energy modulation expected from the experimental parameters used for the particular data set. This is in agreement with particle tracking simulations that predict $\langle M \rangle = 0.45 M_{max}$ when the typical rms timing jitter of 1 ps at this facility is included.

We present three measurements that confirmed the behavior expected from theory. We confirmed the validity of the Lawson-Woodward theorem and verified the expected dependence of the modulation on the laser electric field strength and the laser-polarization angle. The Lawson-Woodward theorem was verified by taking two successive laser time scans, one with the boundary in place and the following with the tape moved out. As shown in Fig. 3, a broadening of the energy spread was observed only when the boundary was present.

The electric field strength dependence was verified by measuring the average modulation strength at different laser beam pulse energies. The laser electric field is proportional to the square root of the laser pulse energy. Figure 4 shows the observed dependence of $\langle M \rangle$ on the peak electric field of the laser. It is observed that the average energy modulation $\langle M \rangle$ varies linearly with the incident laser electric field as expected from theory and shows no significant offset from the origin. The solid line is

the linear fit of the experimental data, and the dashed line is the average modulation from the model. The horizontal dashed line indicates the noise floor limit. The expected peak energy gain at the maximum laser pulse energy is 12 keV, corresponding to 24 keV peak energy modulation. As shown in Fig. 4 the observed average modulation $\langle M \rangle$ at maximum laser power is 14 keV, about $1/2$ of the expected maximum modulation, confirming that $\langle M \rangle \sim \langle M \rangle_{model}$.

Figure 5(b) shows the observed average energy modulation as a function of laser polarization, which is found to be in good agreement with the expected dependence on polarization angle θ. The solid line is the cosine fit of the experimental data, and the dashed line is the noise floor limit. The observed strong dependence on the laser-polarization angle rules out plasma based acceleration
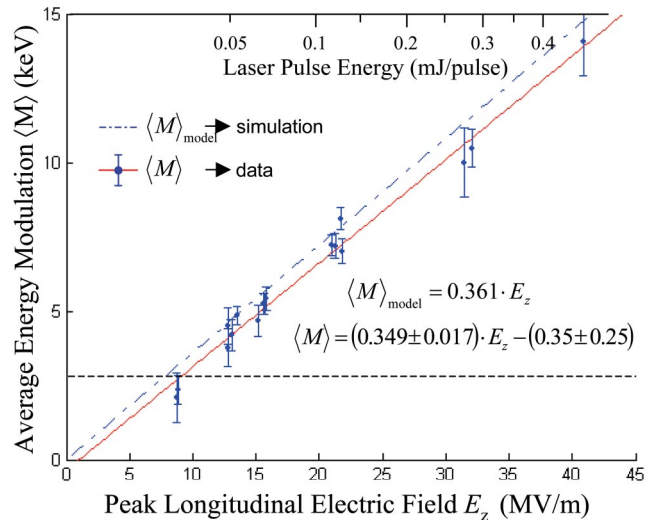

FIG. 4 (color).   Dependence of $\langle M \rangle$ on E_z.

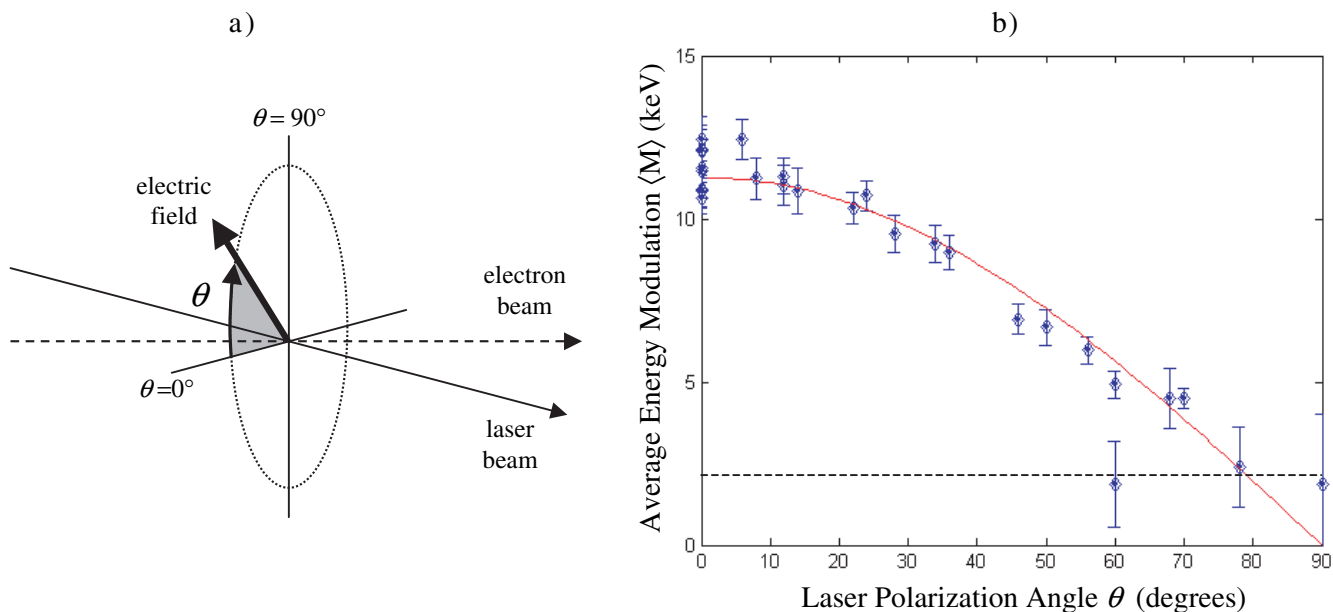a)   b)

FIG. 5 (color).   (a) Diagram of the laser electric field orientation. (b) Dependence of $\langle M \rangle$ on the polarization angle.

mechanisms as significant contributors to the observed energy modulation.

In conclusion, we have observed acceleration of relativistic electrons in vacuum by a properly terminated, linearly polarized laser beam. The observed energy modulation was verified to scale linearly with the longitudinal component of the electric field of the laser, to follow a cosine dependence on the polarization, and in accordance to the Lawson-Woodward theorem to require a boundary to limit the spatial interaction of the incident laser beam with the electron beam. In this first demonstration the experimental parameters were aimed at optimizing the effect from a single interaction in an open experimentally expedient geometry. Future experiments with closed, extended structures will be aimed at improving efficiency and raising the gradient significantly.

[1] W. K. H. Panofsky and M. Breidenbach, Rev. Mod. Phys. **71**, S121 (1999).
[2] J. A. Edinghofer and R. H. Pantell, J. Appl. Phys. **50**, 6120 (1979).
[3] E. Esarey, P. Sprangle, and J. Krall, Phys. Rev. E **52**, 5443 (1995).
[4] J. D. Lawson, IEEE Trans. Nucl. Sci. **26**, 4217 (1979).
[5] R. H. Pantell and M. A. Piestrup, Appl. Phys. Lett. **32**, 781 (1978).
[6] Z. Huang, G. Stupakov, and M. Zolotorev, Phys. Rev. ST Accel. Beams **7**, 011302 (2004).
[7] S. Preuss, A. Demchuk, and M. Stuke, Appl. Phys. A **61**, 33 (1995).